Interdiffusion: fractal structures, scaling, size effect



1990 J. Phys. A: Math. Gen. 23 5309

(http://iopscience.iop.org/0305-4470/23/22/019)

J. Phys. A: Math. Gen. **23** (1990) 5309-5317. Printed in the UK

# Interdiffusion: fractal structures, scaling, size effect

V B Sapozhnikov and M G Goldiner

Centre of Scientific Research, Investigation Automation and Metrology, Moldavian Academy of Sciences, Grosul str. 3/2, Kishinev, USSR

Received 1 March 1990

**Abstract.** Interdiffusion that proceeds via the vacancy mechanism with formation of an ideal substitutional solid solution is investigated by Monte Carlo simulation on a square lattice. The produced stochastic structures studied are the percolation diffusion front and the total boundary of the clusters. It is shown that they have a fractal geometry and that their evolution is characterized by a number of critical exponents. A conclusion is made that the fractal nature of the diffusion front leads to diffusion size effect in thin films. The approach used permits description of propagation of superconducting, conducting, magnetic and other phases during interdiffusion.

## 1. Introduction

The aim of this work is to investigate the geometry of structures produced by interdiffusion in a solid, the laws governing the evolution of these structures and the diffusion size effect caused by the formation of these structures.

Diffusive homogenization gives rise to numerous processes in solids, such as the onset of mechanical stresses, formation and growth of phases, chemical reactions, change of the electric conductivity, etc. These processes are usually described by using the macroscopic characteristics of the diffusive homogenization picture, that is the concentration profile and motion of plane having a constant concentration. It will be shown below, however, that such an averaged description is utterly insufficient, since it bypasses the most important features of the geometry of structures formed in the diffusion zone. These features are connected with the stochasticity of the diffusion process, which makes these structures essentially rough. Yet it is just these features which determine, for example, the kinetics of electric contact-making in diffusion, the change of electric properties of semiconductors following the spreading of the dopant (Mott transition, formation of p-n junction), and also the course of many other processes in solids.

Their effect is particularly large in objects of small size. We have shown that the roughness of such structures plays a vital role in thin films and leads to the diffusion size effect.

The problem is also important in connection with the recent advances in production of high-temperature superconducting materials. The study of geometry and the laws governing the evolution of the superconducting phase obtained by interdiffusion of sinterable components is of great interest.

We have proposed and implemented an approach, different from the macroscopic one, to the description of interdiffusion. It provides a more complete description of

0305-4470/90/225309+09$03.50  

the diffusion picture in the language of scaling structures. The approach proposed is connected with a number of problems concerning the properties of percolation clusters. In contrast to the traditional problems, however, in which the static picture is analysed, we have investigated a case of physical importance (interdiffusion), for which it is essential to know how the percolation picture evolves with time.

So far no attempts have been made to describe interdiffusion with the aid of the formalism used to describe fractal structures. Sapoval *et al* [1] used the algorithm developed to simulate percolation clusters to describe the diffusion picture on a square lattice in the case when the source of the diffusing atoms is an equal-concentration line. Their method is quite rapid and therefore permits analysis of cases of large diffusion length. But it is not fully consistent since it combines macroscopic and microscopic approaches (no direct simulation of diffusion is performed). Its adequacy therefore still remains unclear. In particular, according to this method the probability of the appearance of an atom in a given site depends only on the average concentration ascribed to the layer in which this site is placed, and does not depend at all on the real surrounding of the site. Even if the potential energy of the atom is independent of the surrounding, such an assumption may turn out to be incorrect for the diffusion mechanism in which a correlated jump of a group of atoms takes place (e.g. for a crowdion mechanism).

## 2. Geometry and evolution of a diffusion front

We have investigated, by Monte Carlo simulation, interdiffusion that proceeds via the vacancy mechanism. A square lattice of $100 \times 200$ atoms is divided into two $50 \times 200$ atom sections. In contrast to [1], all the lattice sites are occupied. In one half are located atoms $A$, and in the other atoms $B$. A vacancy moves randomly over the lattice and jumps each time with equal probability to one of the four nearest-neighbour sites.

We designate the lattice boundaries parallel to the interface as, respectively, boundaries $A$ and $B$, and we call the two others the lateral boundaries. Boundaries $A$ and $B$ are reflecting. To decrease edge effects, the two other boundaries are 'joined' (cyclic boundary conditions). After every $10^7$ vacancy jumps we analyse the instantaneous location of atoms $A$ and $B$. During the computer experiment, the vacancy executed $3.6 \times 10^8$ jumps.

We introduce now the concept of a diffusion front (figure 1($a$)). We explain this concept by ascribing to the atoms $A$ and $B$ different electric properties. Let $A$, for example, be metal atoms and $B$ insulator atoms. Let an electric contact between atoms $A$ be realizable via the nearest four neighbours. From the very beginning the outer boundary of the cluster of atoms $A$ electrically connected with the boundary $A$ coincides with the straight line separating the atoms $A$ and $B$. This boundary should be displaced as a whole in the course of diffusion and its shape should change due to the stochasticity of the diffusion process. We shall show that it becomes essentially rough. We call this boundary the percolation diffusion front. In fact the percolation diffusion front is the interphase boundary. It separates the conducting phase from the non-conducting one. (We shall refer henceforth, for brevity, to conducting and non-conducting phases, although the analysis applies equally well to a number of other problems for which the connectivity of atoms is important, e.g. to the propagation of magnetic phases, etc.) The location and form of the front are determined both by the distribution of the atoms over the lattice cites and by the connectivity radius. In our model the connectivity

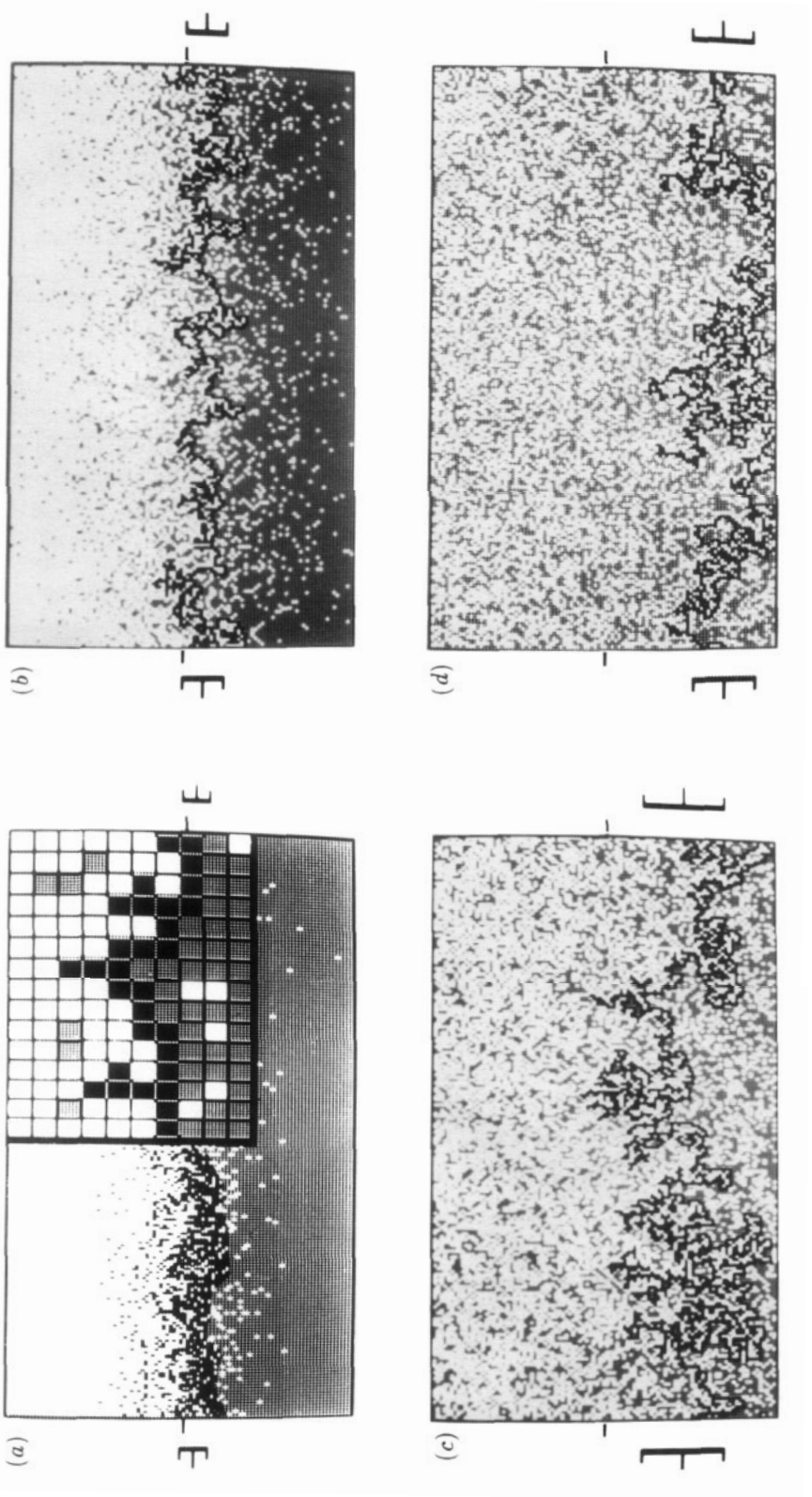


**Figure 1** Diffusion front at different instants of time. The number of vacancy jumps is (*a*) $10^7$, (*b*) $4\times10^7$, (*c*) $2.4\times10^8$ and (*c*) $3.4\times10^8$. Atoms *B* are white toms *A* are grey and the fronts of atoms *A* are black. Magnification of the insert at (*a*) is 70.

radius is equal to unity, since the connection takes place only via nearest neighbours. It can, however, also be larger. Thus for Mott transition the connectivity radius is of the order of Bohr radius, which amounts to tens of lattice periods in semiconductors.

Clearly, the diffusion front geometry and the laws governing its displacement should play the primary role in such processes as diffusion induced contact making or the change of electric properties of semiconductors following the diffusion of a dopant. These are, in fact, the diffusion front characteristics studied by us.

We have shown that diffusion front is a line with dead ends and we have proved that it has no self-crossing.

The form of the front at various instants of time is shown in figure 1. The geometrical scale properties of the front were investigated by two methods: (1) the front length $L(\lambda)$ was measured with different step lengths $\lambda$; (2) we then obtain for different values of $d$ the average number $N(d)$ of front points inside a circle of diameter $d$ drawn around the front point. These plots after $2.4\times10^8$ vacancy jumps are shown in figure 2, from which it is seen that the diffusion front is a fractal up to a scale of about 40. The values of the fractal dimension were determined for various instants of time from the relations $L(\lambda)\propto\lambda^{1-D_L}$ and $N(d)\propto d^{D_N}$. Both $D_L$ and $D_N$ have a weak tendency to increase with time against the background of the fluctuations. During the computer experiment $D_L$ rose from $1.56\pm0.02$ to $1.67\pm0.02$, and $D_N$ from $1.48\pm0.01$ to $1.60\pm0.01$. The inequality $D_L > D_N$ was satisfied at each instant of time, since the dead ends were taken into account in the determination of $D_L$.

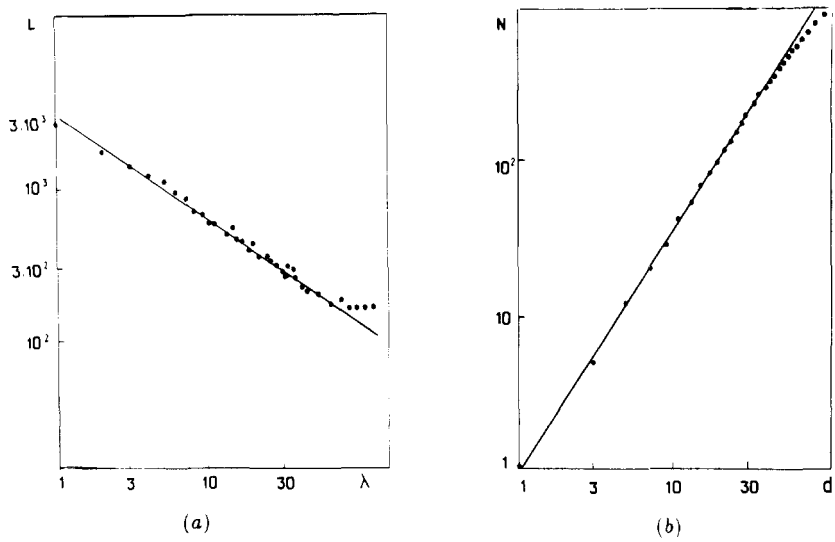


**Figure 2.** Diffusion front scaling after $2.4\times10^8$ vacancy jumps.

For each analysed front we determined also the distribution of the front points over layers parallel to the boundaries $A$ and $B$, the shift $x_F$ of the average front position and the mean squared displacement from the central position, $\sigma_F$, which characterises the front width. The distribution of the front points over the layers turned out to be close to Gaussian (figure 3).

In the course of diffusion the front of atoms $A$ moved to the boundary $A$. We investigated the time evolution of the front characteristics. As seen from figure 4, the

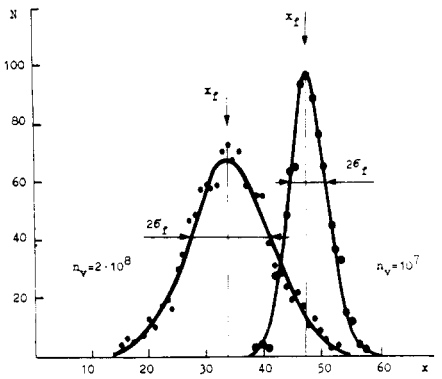


**Figure 3.** Front atom distribution ($N$) over the layers ($n$) at different instants of time.

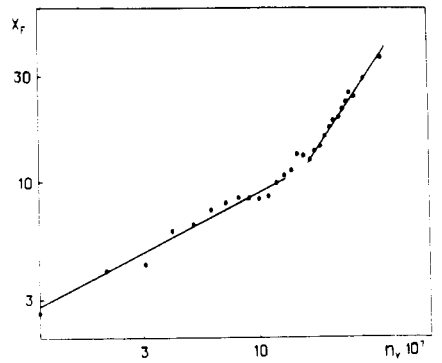


**Figure 4.** Displacement of average position of front upon interdiffusion.

front motion was given initially by $x_F \propto t^{0.51\pm0.03}$ and later by $x_F \propto t^{1.5\pm0.03}$. The second regime was set in because the diffusion became such that the limited size of the lattice came into play. The value of the critical exponent in the first regime, corresponding to diffusion in semi-infinite sample, suggests that the exponent is exactly equal to 0.5. This means that the average front position moves like a line of constant concentration $c_F$.

To continue the analysis we introduce the diffusion length $l_D = 2(Ft)$, where $F$ is the diffusivity of the sample. For diffusion by the vacancy mechanism on a square lattice the diffusivity is $F = fcw/4$, where $c$ is the vacancy concentration, $w$ is the frequency of the vacancy jumps and $f \approx 0.465$ is the correlation factor. Hence $l_D = (fn/N)$, where $n$ is the number of vacancy jumps and $N$ is the number of lattice sites.

Assuming that in the first regime the critical exponent for $x_F$ is exactly 0.5, we get

$$x_F = -(0.18 \pm 0.02) l_D \propto t^{0.5}. \tag{1}$$

The width of front had a power-law growth

$$\sigma_F \propto l_D^{\alpha_\sigma} \qquad \alpha_\sigma = 0.58 \pm 0.05. \tag{2}$$

The number $N_F$ of atoms belonging to the front also increased with time $t$. This growth, however, was against the background of strong fluctuations, so that it was impossible to determine the $N_F(l_D)$ dependence reliably from the computer experiment.

It is nevertheless easy to show that this dependence should also follow a power law. Indeed, since the front is a fractal up to scales $\propto\sigma_F$, it can be represented as a linear chain consisting of squares $\propto\sigma_F$ on the side, with the front fractal inside each square. The number of such squares is $\propto\sigma_F^{D_N}$ and the number of atoms in each square is $\propto\sigma_F^{D_N}$. Hence

$$N_F \propto \sigma_F^{D_N-1} \propto l_D^{\alpha_\sigma(D_N-1)}$$
$$N_F \propto l_D^{\alpha_N} \qquad \alpha_N = \alpha_\sigma(D_N-1). \tag{3}$$

The values of fractal dimension in our case are somewhat lower than in [1], where a value $D_N = 1.76 \pm 0.02$ was obtained for a diffusion length $l_D = 12\,800$. This is seemingly due to the fact that our lattice was smaller. Indeed, in [1] the fractal dimension for $l_D = 50$ is $D_N = 1.62$. The concentration on the average line of front, and also the values of the critical exponents for $x_F$ and $\sigma_F$, agree with data of [1], where it is shown also that $\alpha_\sigma = \nu/(\nu+1) \approx 0.571$ ($\nu = \frac{4}{3}$ is the critical exponent of percolation theory). The difference between the factors preceding the power is due to the different initial and boundary conditions.

Since, as noted above, the average position of the front at each instant coincides with the line of constant concentration $c_F$, the question of value and meaning of this concentration arises. From general consideration one can expect it to be close to the critical concentration $c_p \approx 0.593$ of percolation on a square lattice [2]. With the aid of the relation $c_F = 0.5\,\mathrm{erfc}(x_F/l_D)$ we obtain from (1)

$$c_F = 0.60 \pm 0.01. \tag{4}$$

It can thus be regarded as established that $c_F = c_p$ within the limits of error. This results agrees with that of [1]. Assume that the relation $c_F = c_p$ holds for all types of lattice. This suggests some conclusions regarding the front evolution. Since $c_p = 0.593$ in our case, and the plane $c = 0.5$ is immobile, the front moves away from its initial position to 'its own' lateral boundary. Therefore in the case of two semi-infinite samples having a square lattice no electric contact is produced during diffusion. On the contrary, connectivity is lost in the sample. For a triangular lattice we have $c_F = c_p = 0.5$ [3]. This means that the line of the front will not move as a whole. A contact should be made, however, as a result of the front's own expansion which is characterized by the function $\sigma_F(t)$.

## 3. Diffusion size effect

Analysis of the percolatiaon diffusion front thus permits a new look at the laws governing the variation of electric and magnetic properties of a body caused by diffusion. For large diffusion length, when $x_F \gg \sigma_F$, the contact is produced at an instant when the $x_F$ plane, having a concentration $c_p$, reaches the opposite boundary. At small lengths of diffusion zone, when $\sigma_F$ is compatible with $x_F$, it must be taken into account that the front has a width $\sigma_F$ of its own, so that to make contact it is sufficient that the plane $\chi_F + k\sigma_F$ reaches the opposite boundary, where $k$ is the certain coefficient of order unity. For a description of the development of the diffusion front it is important that $x_F$ and $\sigma_F$ have different time dependencies. Indeed, in a macroscopic description the diffusion in an unbounded solid is a self-similar problem, since the diffusion picture is determined completely by a dimensionless variables $x/(Ft)^{1/2}$. When diffusion is described in terms of diffusion front, it becomes clear that the problem is not self-similar

for small diffusion lengths. It becomes self-similar only in the limit of large lengths, when $\sigma_F \ll x_F$, that is $l_D < 10^3$. In such cases the problem is said to be incompletely self-similar. The incomplete self-similarity found means that the diffusion size effect caused by the fractal nature of the diffusion front takes place in solids.

Since the values of front shift and front length fluctuate strongly, one should also expect electric-resistance fluctuations (noise) at the instant of contact making in small samples.

It should be noted that in thin films there may be observed other diffusion size effects. For example, we have predicted [4] and experimentally confirmed [5] the existence of the diffusion size effect caused by the particularities of the crystal lattice dynamics near surface.

## 4. Geometry and evolution of the total boundary of clusters

Besides the diffusion front, we have investigated also the geometry and the evolution of the total boundary between all produced clusters of atoms *A* and *B*. This boundary is defined as the aggregate of bounds of type *AB*. It is just on this boundary that the mixing energy of atoms *A* and *B* ($\varepsilon = \varepsilon_{AB} - 0.5\varepsilon_{AA} + \varepsilon_{BB}$, where $\varepsilon_{AA}$, $\varepsilon_{BB}$ and $\varepsilon_{AB}$ are the binding energies of the corresponding atom pairs) is localized. It is therefore of interest to study the geometry and the time evolution of this boundary.

In our model the probability of a vacancy jump in one or another direction does not depend on the surrounding. This corresponds to the limiting case $\varepsilon \ll kT$. Clearly, the front is related to the total boundary of clusters just as the continental shore line is related to the shore line that includes also the shores of islands and lakes [6]. The dimension $D_b$ of total boundary of the clusters comes close to two. Thus, $D_b = 1.91 \pm 0.01$ after $10^7$ vacancy jumps and $D_b = 1.97 \pm 0.01$ after $2 \times 10^8$ jumps (figure 5). This means that in the limit of large diffusion lengths the boundary is the space-filling fractal. This corresponds to the results obtained by solving the percolation problem

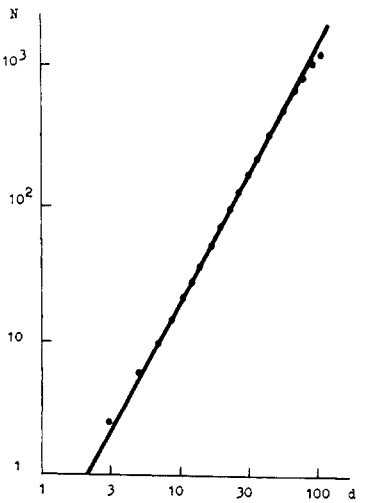


**Figure 5.** Scaling of the total boundary of clusters formed upon interdiffusion after $2 \times 10^8$ vacancy jumps.

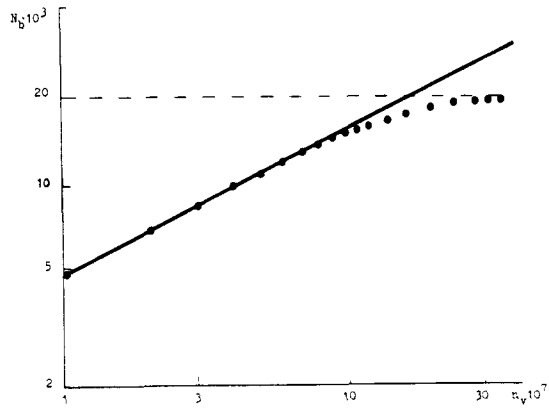


**Figure 6.** Length of the total boundary of clusters formed upon interdiffusion.

in [6, 7] where it is shown that the fractal dimension of the total boundary of clusters is equal to two.

The number $N_b$ of atoms of total boundary increases as a power law (see figure 6): $N_b = (320 \pm 10) l_D^{0.98 \pm 0.02}$. This suggests that the critical exponent for $N_b$ is equal to unity. Then

$$N_b = (1.60 \pm 0.01) l l_D \propto t^{0.5}. \tag{5}$$

The total alloy-mixing energy is therefore

$$E = N_b \varepsilon = (1.60 \pm 0.01) l l_D \varepsilon \propto t^{0.5}. \tag{6}$$

The relation (5) suggests that the population of lattice site is independent on its surrounding in our case. Indeed, if this assumption is correct we get, recognising that $c(x) = 0.5 \operatorname{erfc}(x/l_D)$, and the number of nearest neighbours is four,

$$N_b = 4l \int_{-\infty}^{\infty} c(x)(1 - c(x))\, dx = (8/\pi)^{1/2} l l_D \simeq 1.60 l l_D \tag{7}$$

which correspond to (5).

## 5. Conclusions

The computer simulation and the analysis lead to the following conclusions

(1) The geometry and the laws governing the evolution of a percolation diffusion front determine the kinetics of the diffusion growth of the phase for which the presence of connectivity (conductive, superconductive, magnetic, etc.) Between definite types of atoms is essential. The diffusion front is the boundary of such phases.

(2) The diffusion front is characterized by a fractal geometry, and its evolution is described by a number of critical exponents.

(3) The fractal nature of the diffusion front causes the diffusion size effect in solids.

(4) In small samples the kinetics of electric contact making is determined not only by the kinetics of displacement of the front as a whole, but also by kinetics of the increase of its width.

(5) The evolution of the diffusion front is of fluctuating type and this should lead in small samples to fluctuations of the corresponding characteristics (e.g., of the electric resistance at the instance of contact making).

(6) The fractal dimension of the total boundary of the clusters formed in the diffusion zone tends with time to two.

## Acknowledgments

The authors thank Professor V L Pokrovsky, Dr S P Obukhov and Dr V I Nikora for most helpful remarks.

## References

[1] Sapoval B, Rosso M and Gouyet J F 1985 *J. Physique Lett.* **45** L149
Sapoval B, Rosso M, Gouyet J F and Colonna J F 1986 *Solid State Ionics* **18** and **21**; **19**
[2] Djordjevic Z F, Stanley H E and Margolina A 1982 *J. Phys. A: Math. Gen.* **15** L405
[3] Sykes M F and Essan J W 1963 *Phys. Rev. Lett.* **10** 3
[4] Sapozhnikov V B, Goldiner M G 1984 *Thin Solid Films* **111** 183
[5] Goldiner M G, Sapozhnikov V B, Meinel K and Klaua M 1990 *Thin Solid Films* to be published
[6] Mandelbrot B B *The Fractal Geometry of Nature* 1982 (San Francisco: Freeman)
[7] Voss R F 1984 *J. Phys. A: Math. Gen.* **17** L373